UPC2025: The second international workshop on the physics of Ultra Peripheral Collisions
June 9-13, 2025

Investigating Spin Interference in photonuclear $\gamma A \rightarrow \pi^+\pi^-$ and $\gamma\gamma \rightarrow \pi^+\pi^-$ at STAR

Samuel Corey
for the STAR Collaboration

Supported in part by
U.S. DEPARTMENT OF ENERGY | Office of Science
THE OHIO STATE UNIVERSITY

STAR

Motivation

- In Ultraperipheral Collisions (UPCs), $\pi^+\pi^-$ primarily from $\gamma A \rightarrow X \rightarrow \pi^+\pi^-$.
- $\gamma\gamma \rightarrow \pi^+\pi^-$ not yet measured in hadronic systems.
- $\gamma\gamma \rightarrow \pi^+\pi^-$ makes up tiny fraction of overall $\pi^+\pi^-$ cross section.

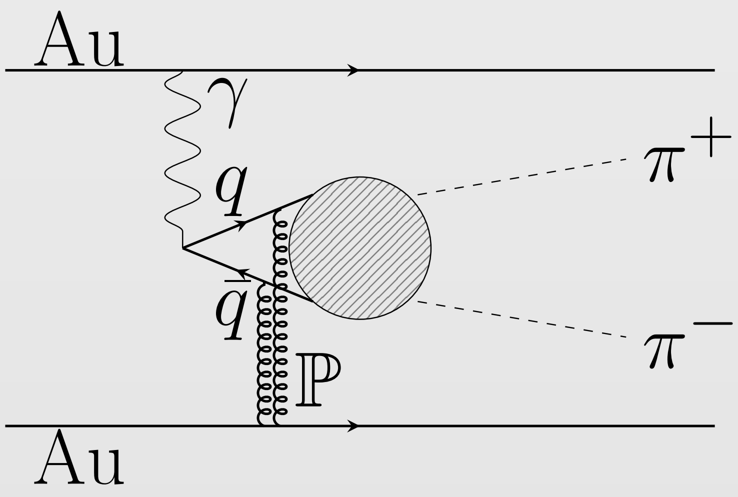

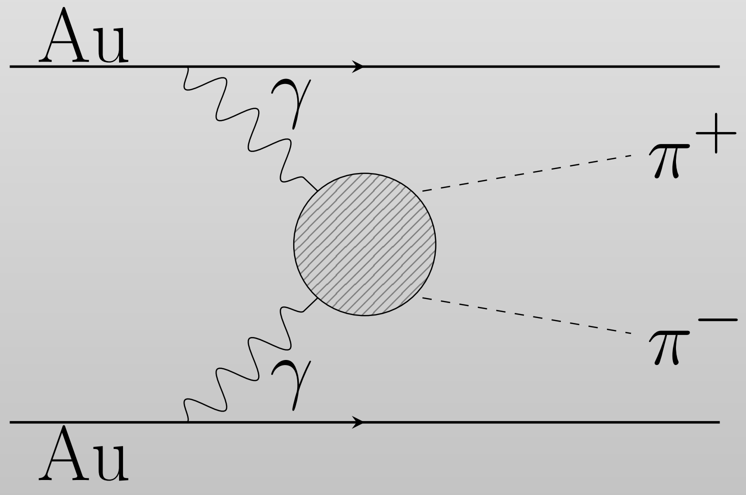

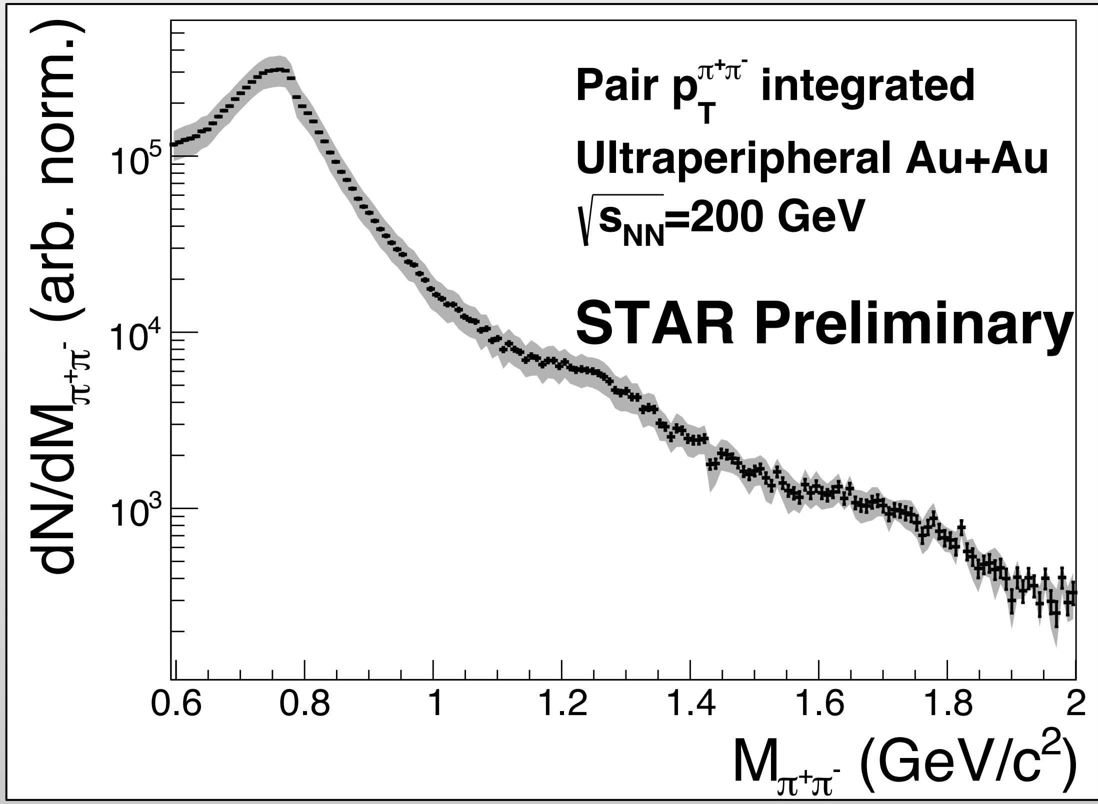

Inclusive distribution

Hadronic Light-by-Light and a_μ

- Hadronic light-by-light (HLbyL) is one the two dominant theoretical uncertainties on a_μ.
- Related to $\gamma\gamma \rightarrow \pi^+\pi^-$ by the optical theorem.
- Previous measurements of $\gamma\gamma \rightarrow \pi\pi$ are from e^-e^+ collisions.
- In UPC, we have quasi-real photons and larger mass range

Melo-Porras et al., Particles 2024, 7(2), 327 – 381

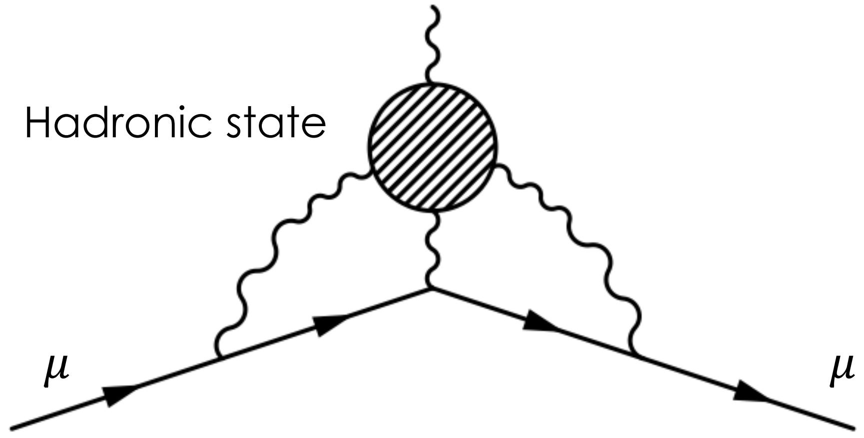

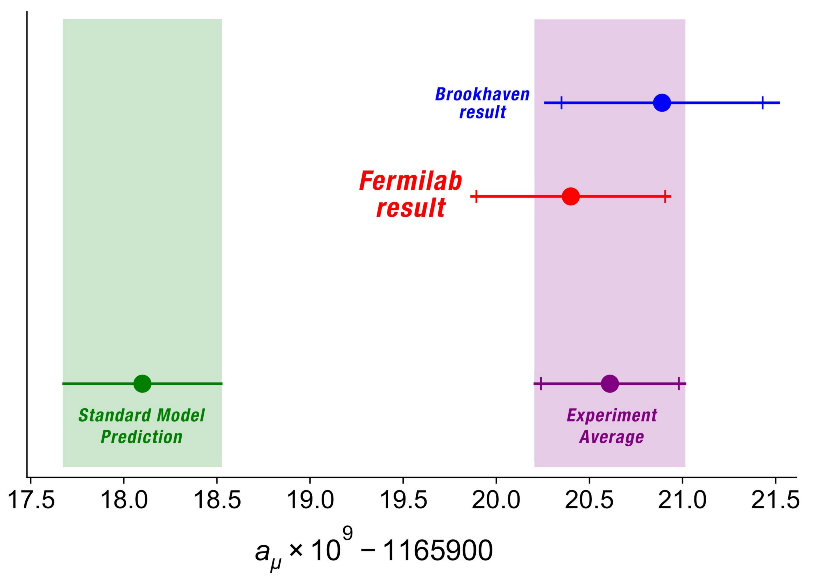

First Results from Fermilab's Muon g-2 Experiment Strengthen Evidence of New Physics; Fermilab, 7 April 2021.

Hadronic Light-by-Light and a_μ

- Hadronic light-by-light (HLbyL) is one the two dominant theoretical uncertainties on a_μ.
- Related to $\gamma\gamma \rightarrow \pi^+\pi^-$ by the optical theorem.
- Previous measurements of $\gamma\gamma \rightarrow \pi\pi$ are from e^-e^+ collisions.
- In UPC, we have quasi-real photons and larger mass range

Danilkin et al. Prog. Part. Nucl. Phys. 107, 20 (2019)

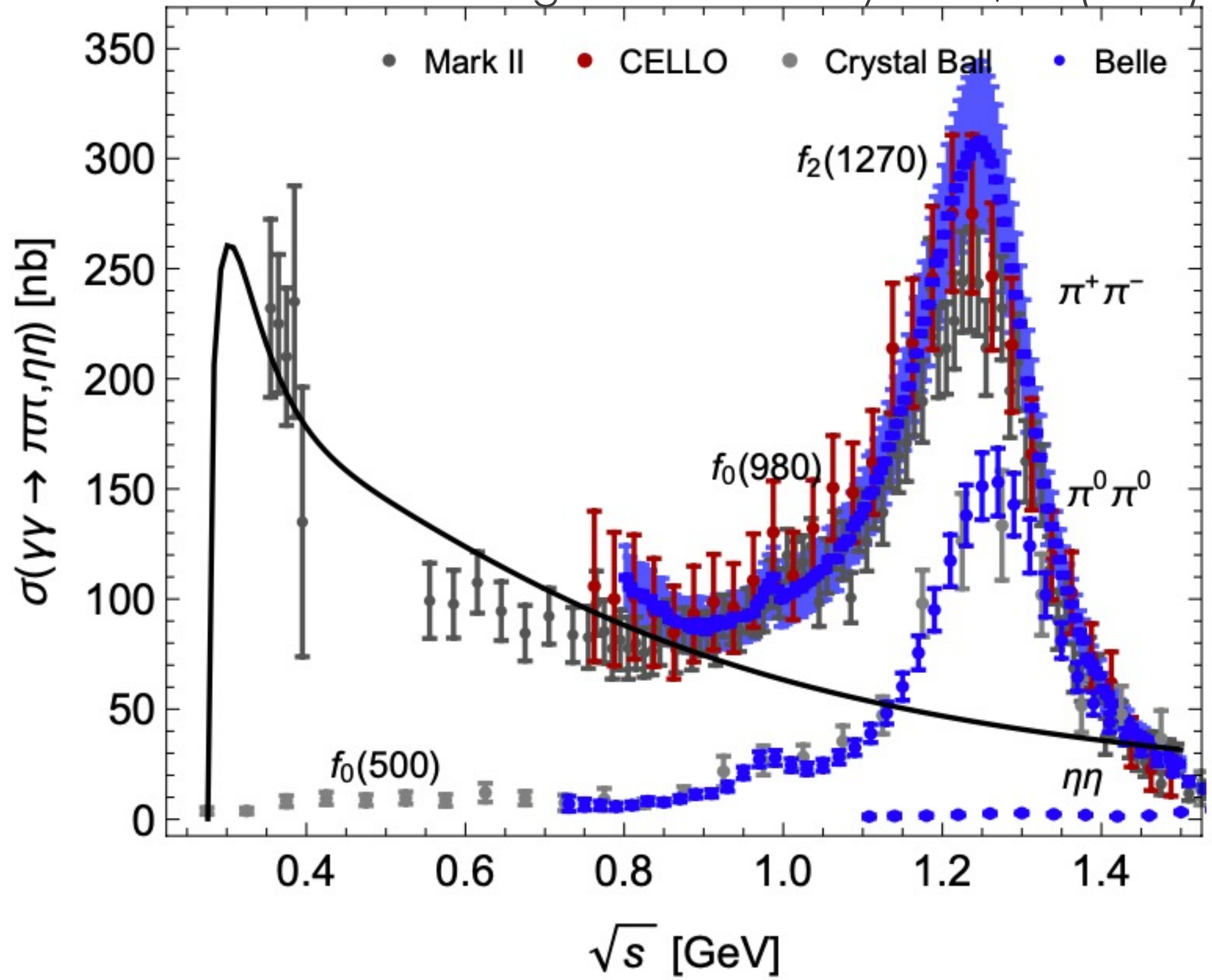

Spin Interference in UPCs

- In γA events, one nucleus acts as the emitter and the other as the target.
- Double slit-like interference leads to a $\cos(2\Delta\phi)$ angular anisotropy.

$$P_{\perp} = p_T^{+} + p_T^{-}$$
$$Q_{\perp} = \frac{1}{2}(p_T^{+} - p_T^{-})$$

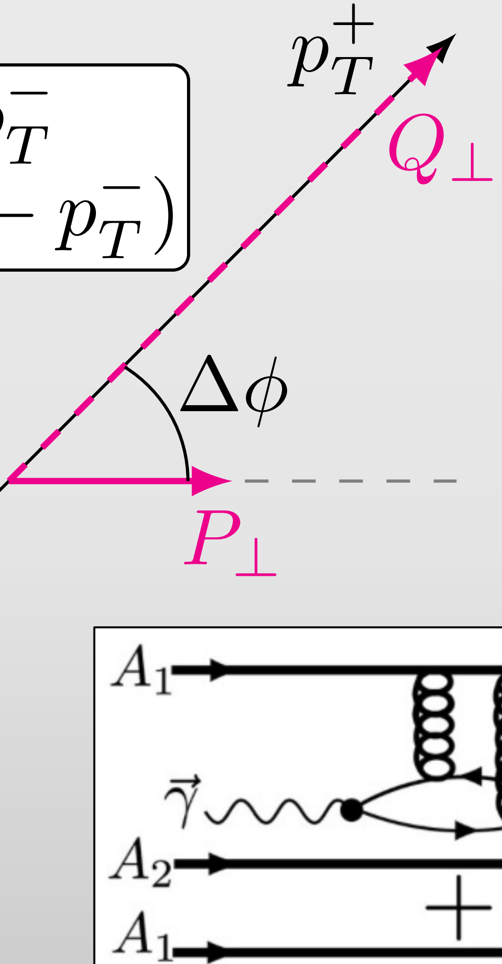

(Brandenburg et al., Phys. Rev. Research 7, 013131 (2025))

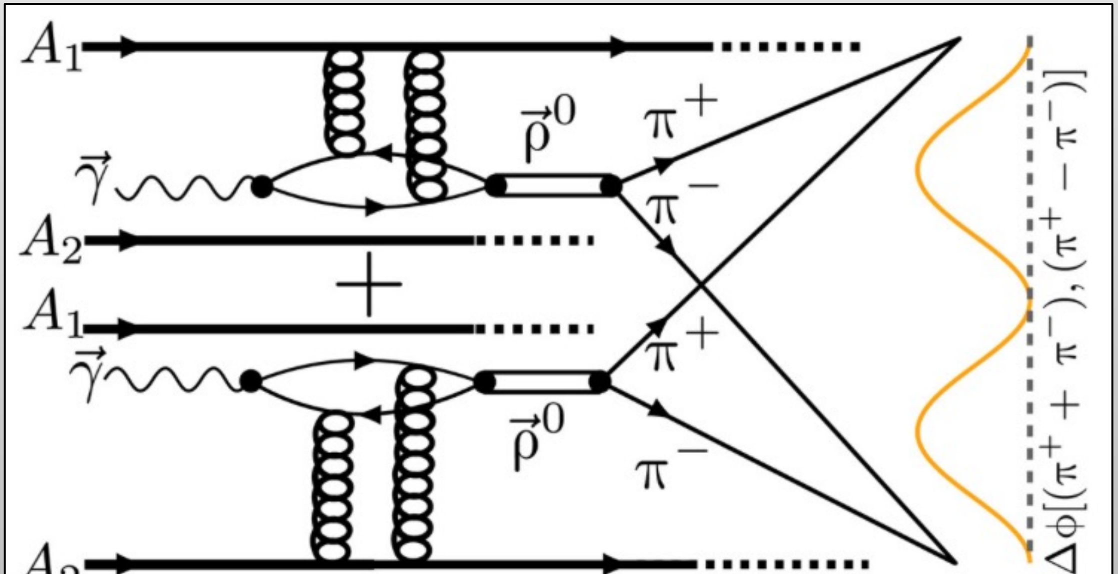

STAR, Sci.Adv.9,eabq3903 (2023)

Previous $\langle 2\cos(2\Delta\phi)\rangle$ measurement

- Photon spin encodes into final state orbital angular momentum: $\cos(2\Delta\phi)$ modulation.
- Present in A+A, but not p+A--photon emission scales with Z^2

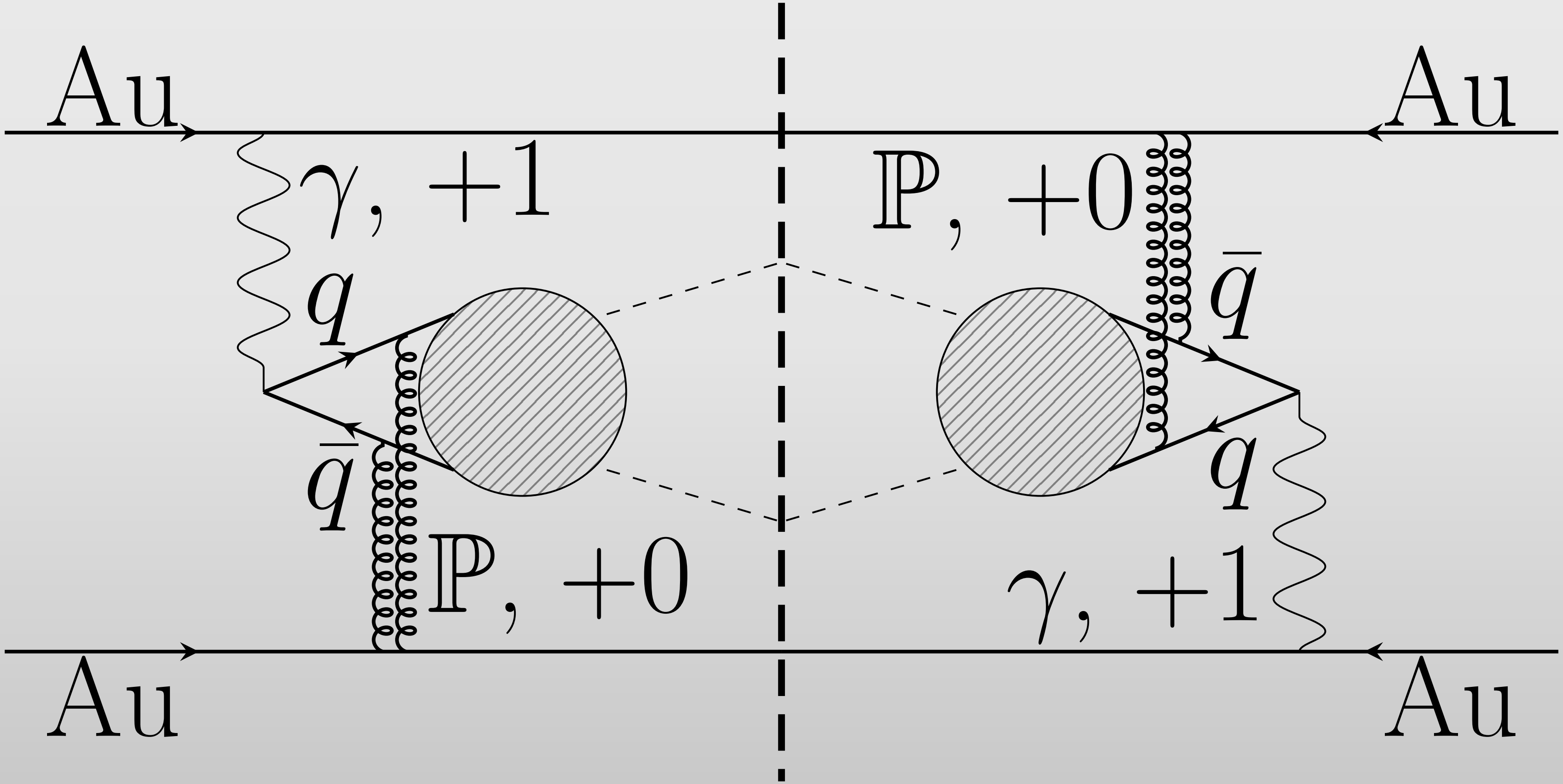

Previous $\langle 2\cos(2\Delta\phi)\rangle$ measurement

- Photon spin encodes into final state orbital angular momentum: $\cos(2\Delta\phi)$ modulation.
- Present in A+A, but not p+A--photon emission scales with Z^2

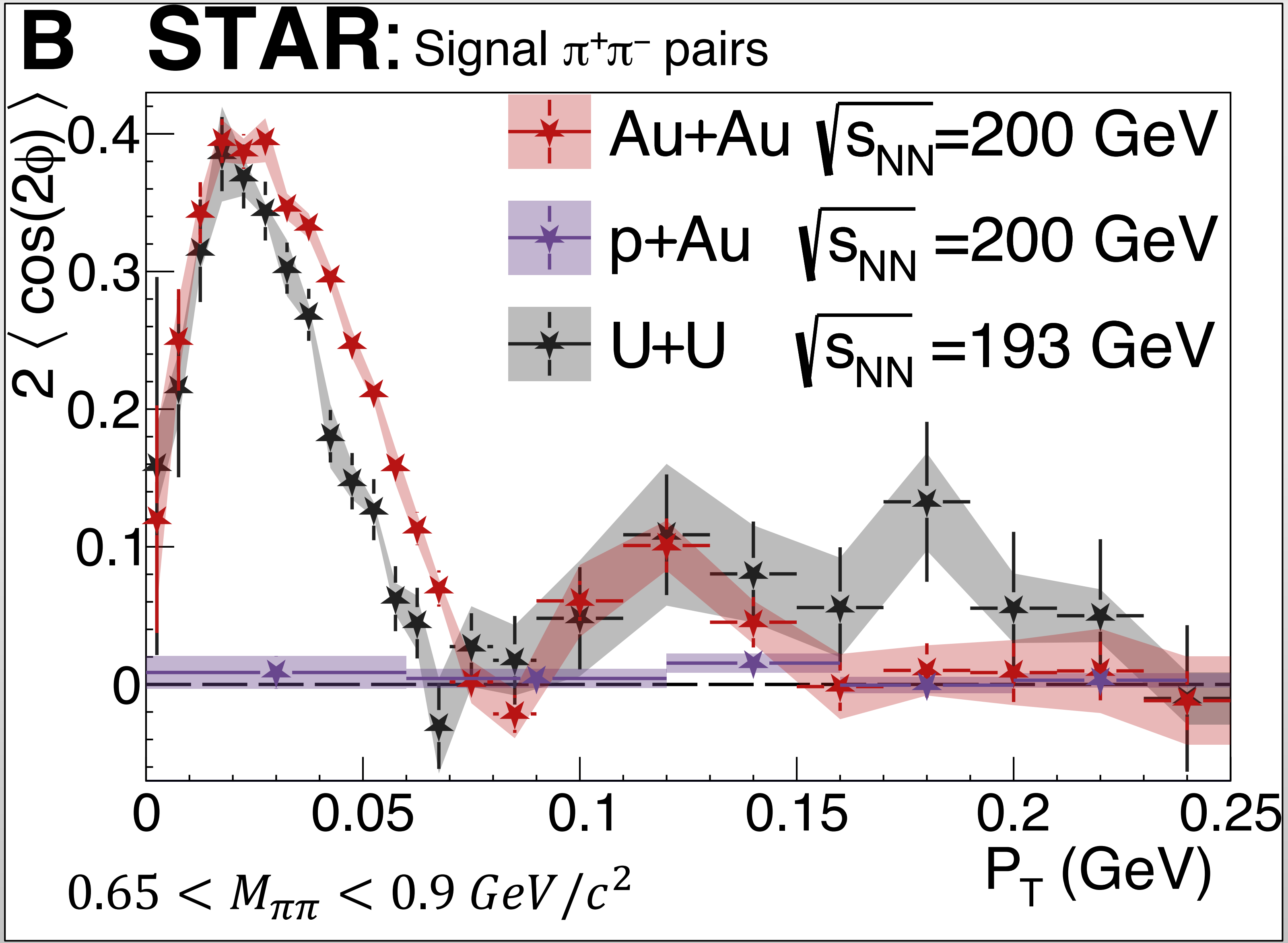

STAR, Sci.Adv.9,eabq3903 (2023)

Spin Interference between γA and $\gamma\gamma$

- Interference between γA and $\gamma\gamma$ also present.
- This interference is expected to produce a $\cos(\Delta\phi)$ and $\cos(3\Delta\phi)$ anisotropy.

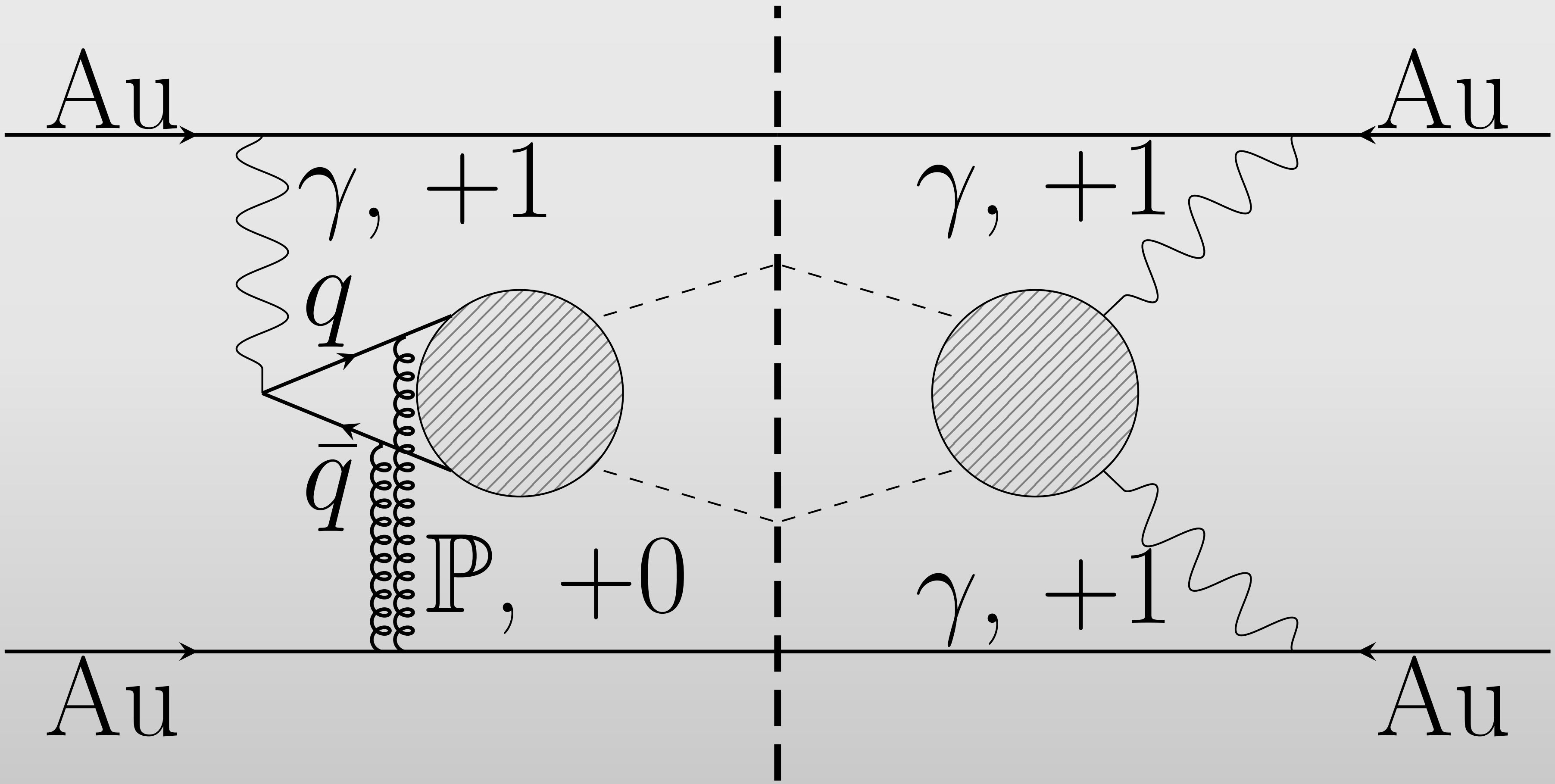

Δϕ distribution

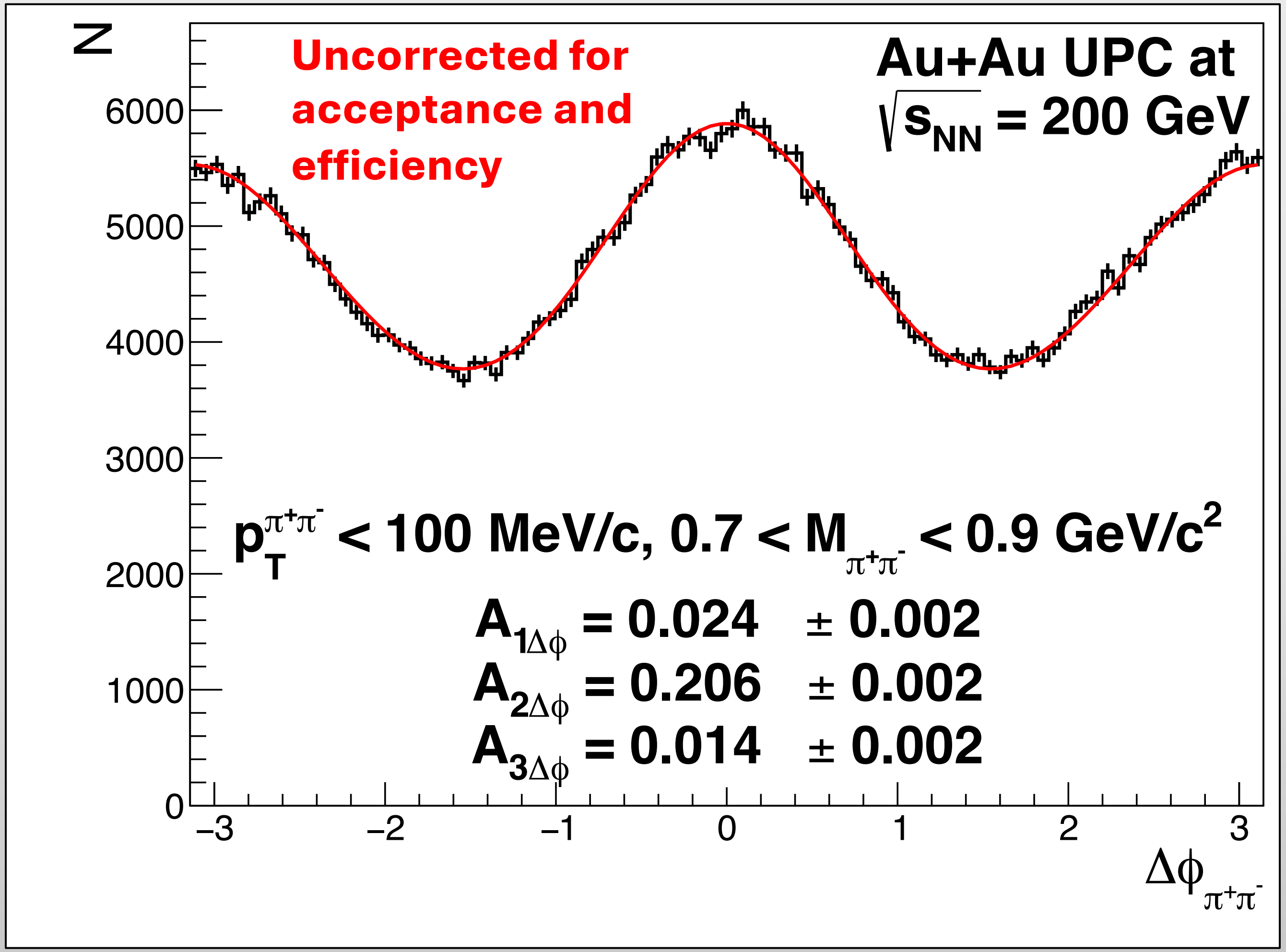

- Uncorrected $\Delta\phi$ distribution fit with:

$$C[1 + A_{1\Delta\phi}\cos(\Delta\phi) + A_{2\Delta\phi}\cos(2\Delta\phi) + A_{3\Delta\phi}\cos(3\Delta\phi)]$$

- Large and highly significant $A_{2\Delta\phi}$.
- $A_{1,3\Delta\phi} \neq 0$: first hint that we have $\gamma\gamma \to \pi^+\pi^-$.

$\Delta\phi$ efficiency and acceptance correction

- Want to measure $A_{n\Delta\phi} = \langle 2\cos(n\Delta\phi)\rangle$ as a function of $p_T, M_{\pi\pi}$.
- $\Delta\phi$ has unique $p_T, M_{\pi\pi}$-dependent acceptance effects.

Example:
High p_T ρ^0

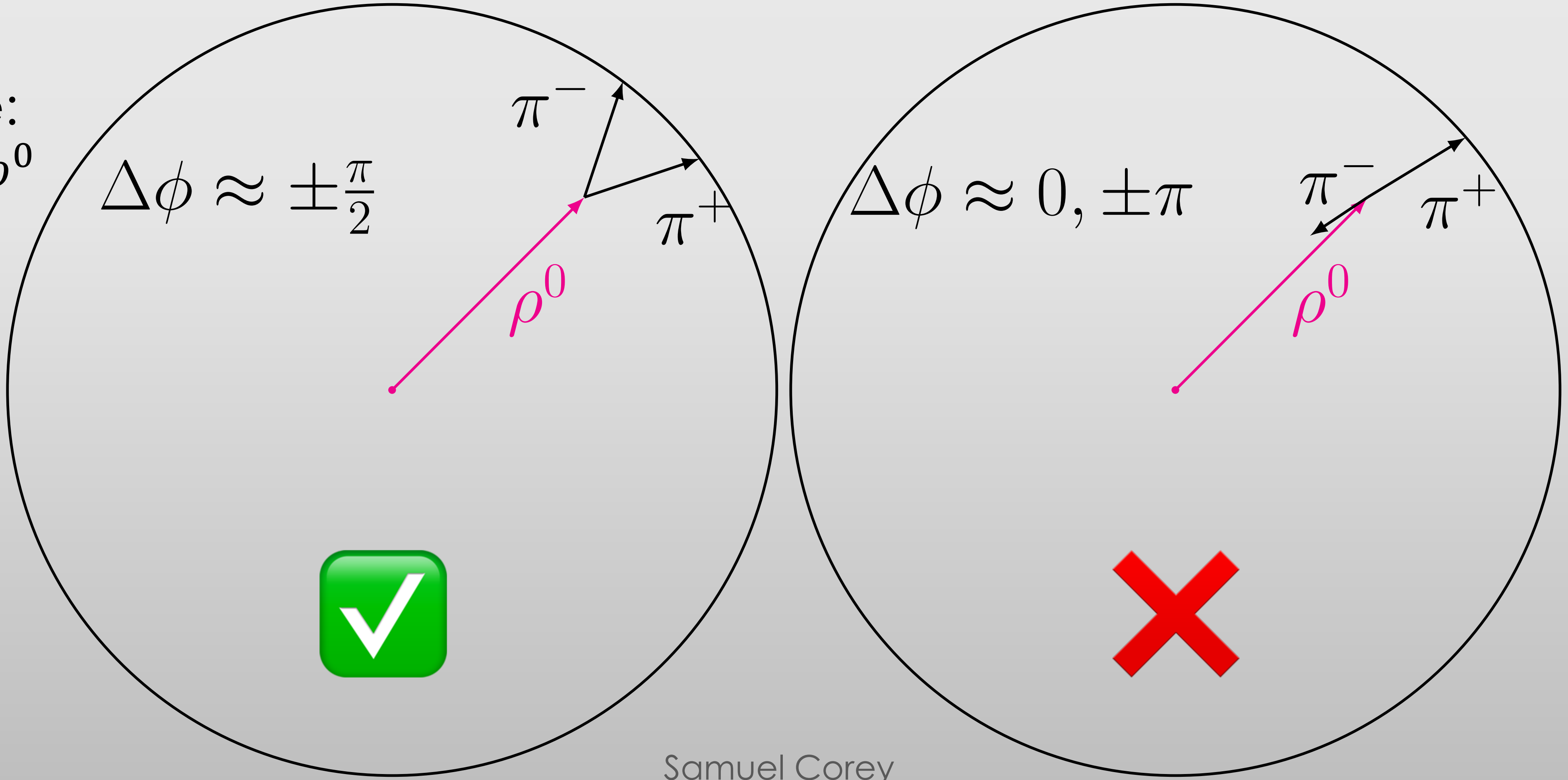

$\Delta\phi$ efficiency and acceptance correction

- Consider γ, α, ω as measured, true, and distortion $A_{n\Delta\phi}$ respectively.

$$\gamma_n = \frac{\int_{-\pi}^{\pi} \alpha(\Delta\phi)\omega(\Delta\phi)\cos(n\Delta\phi)\, d\Delta\phi}{\int_{-\pi}^{\pi} \alpha(\Delta\phi)\omega(\Delta\phi)\, d\Delta\phi}$$

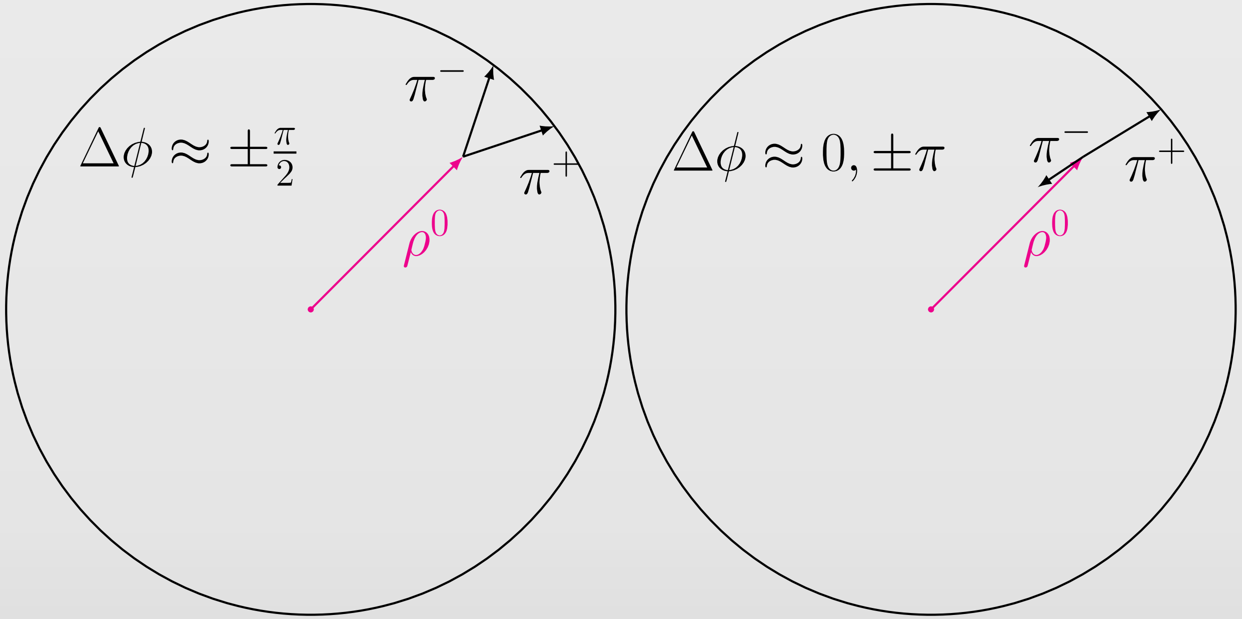

- Expand $\alpha(\Delta\phi), \omega(\Delta\phi)$ as Fourier series, and assume only one term nonzero.

- Computing integral and inverting for α_n leaves:

$$\alpha_n = \frac{-2(\gamma_n - \omega_n)}{\gamma_n \times \omega_n - 2}$$

$\langle 2\cos(2\Delta\phi)\rangle$ vs. $M_{\pi\pi}$

- ω_n calculated with toy model using STAR acceptance.
- Correction applied in each bin in $p_T, M_{\pi\pi}$, then projected.

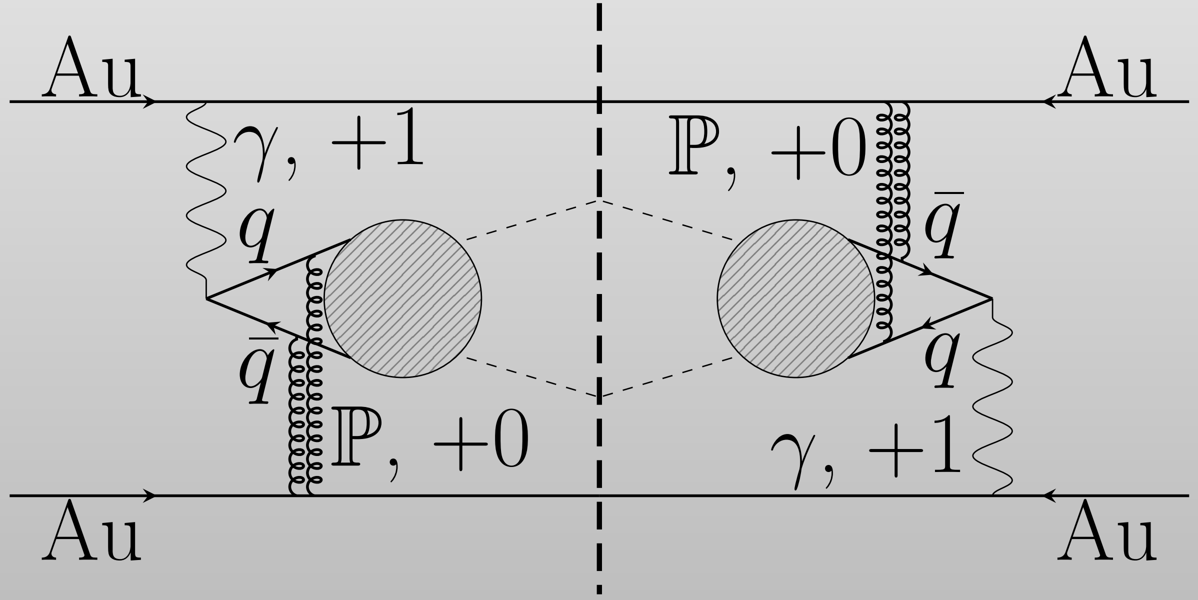

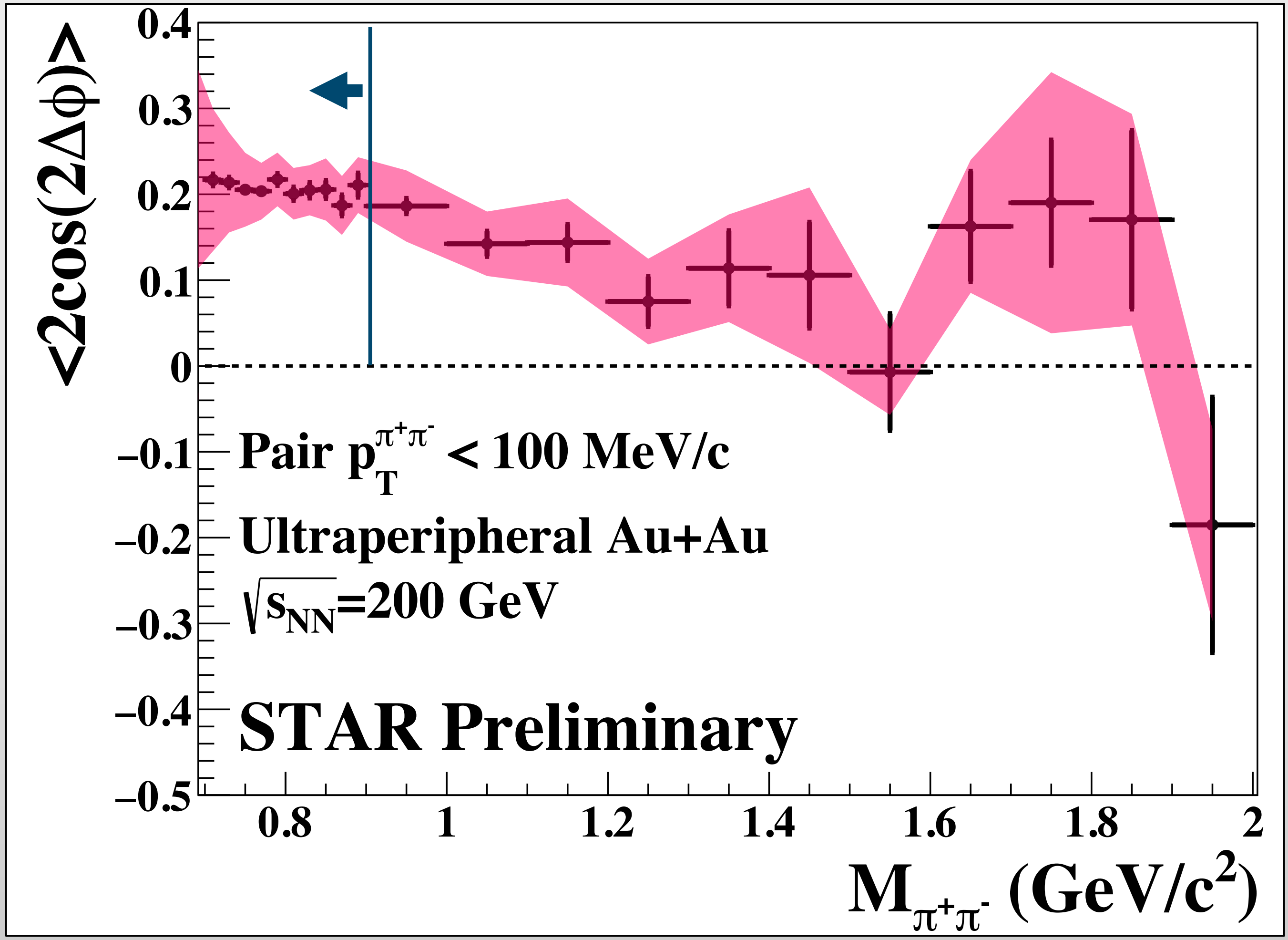

Left of solid line: previous STAR result

⟨2cos(1,3Δϕ)⟩ measurement

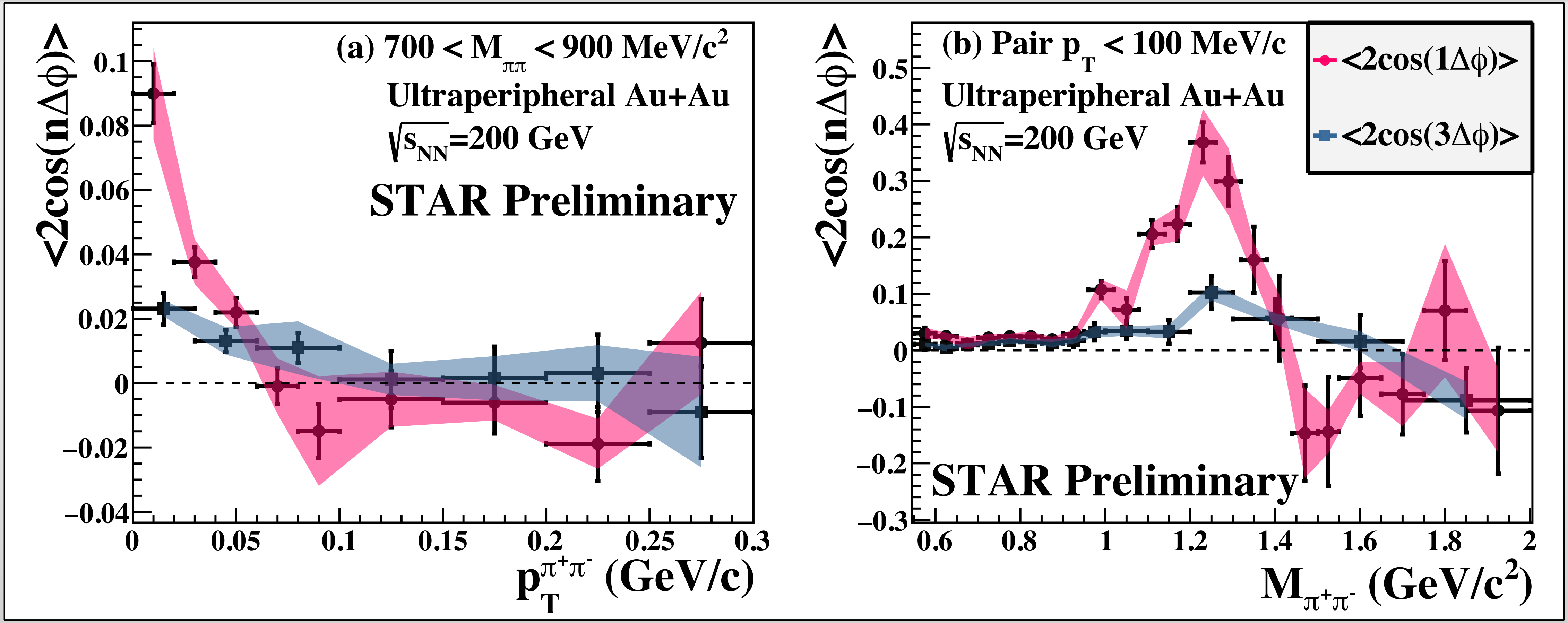

- Interference between $\gamma A \to \rho^0 \to \pi^+ \pi^-$ and non-resonant $\gamma\gamma \to \pi^+ \pi^-$ near ρ^0 mass.
- Large feature near 1270 MeV/c^2: $\boldsymbol{f_2(1270)}$ **resonance**

UPC 2-pion invariant mass distribution

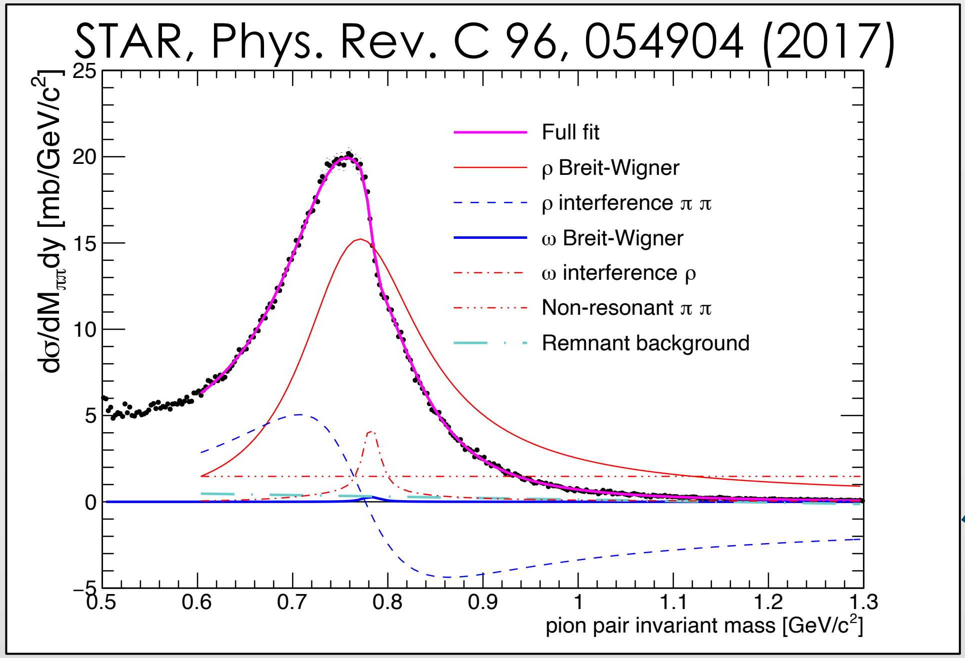

- To apply this to this analysis' mass range, we need to add **two more resonances**

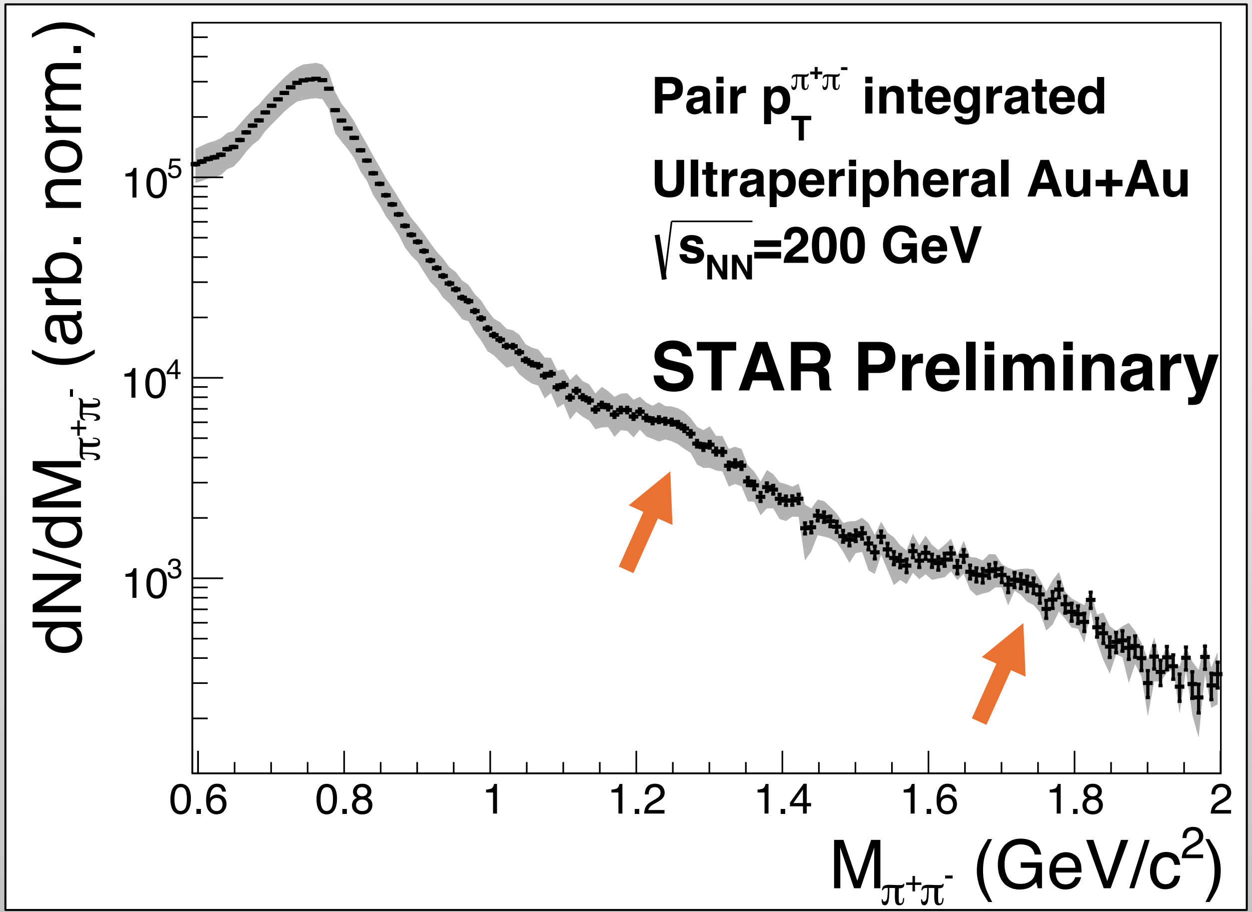

- Previous STAR fit includes:

$$|\rho^0 + \omega + B_{\pi\pi}|^2$$

- Where $B_{\pi\pi}$ is the Drell-Söding process, modeled by a constant.

- The interference terms are very important to determine the shape.

Including spin information

- Without spin information, nature of higher resonances is ambiguous.
- Examples:
  - $f_2(1270)$ vs. $\rho(1450)$
  - $\rho(1700)$ vs. $\rho_3(1690)$
- Including $\Delta\phi$ information allows us to differentiate these.

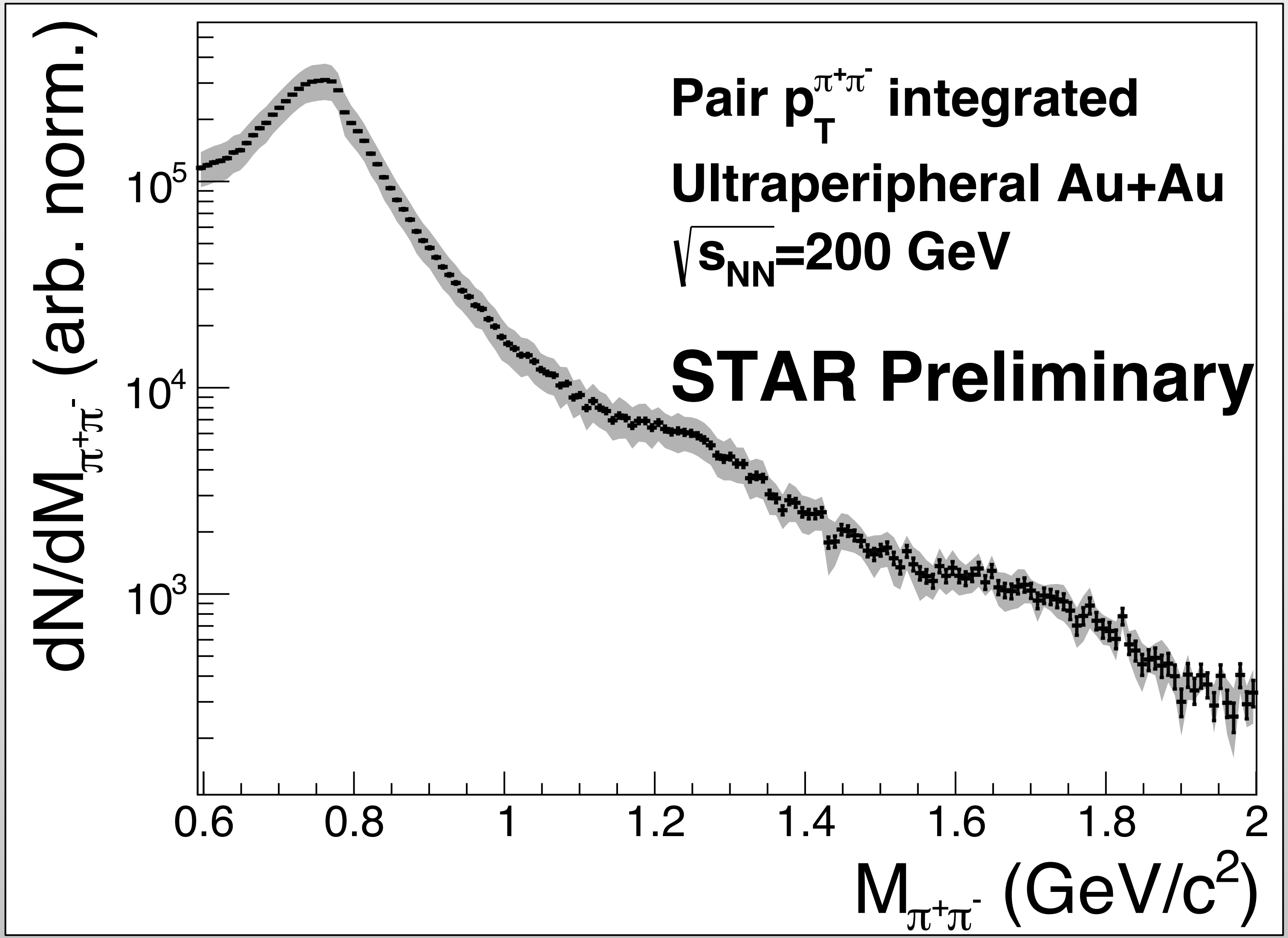

Describing $\langle 2\cos(n\Delta\phi)\rangle$ vs. $M_{\pi\pi}$

- Consider the UPC $AA \rightarrow AA\pi^+\pi^-$ cross section as:

$$\propto |\rho^0 + \omega + f_2(1270) + \rho(1700) + B_{\pi\pi}|^2$$

- Each cross term contributes to $A_{n\Delta\phi} \equiv \langle 2\cos(n\Delta\phi)\rangle$ according to the spin of the interfering states.

- Assume that **each cross term contributes a constant value, and the observed $A_{n\Delta\phi}$ is the average of these constants** weighted by the contribution of that term to the total cross section.

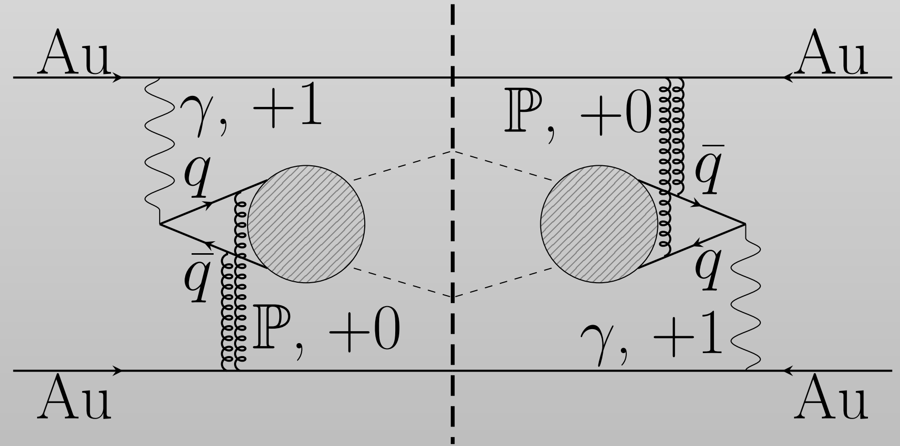

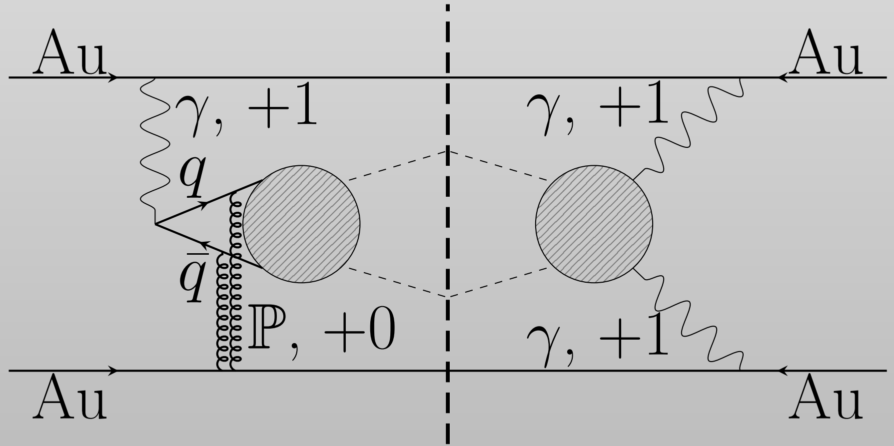

Simultaneous Fit Procedure

- In this formulation, fit the invariant mass spectrum, $A_{1\Delta\phi}$, $A_{2\Delta\phi}$, and $A_{3\Delta\phi}$.

- $$\frac{d\sigma}{d\mathrm{M}_{\pi\pi}} = \left| \frac{A_\rho \sqrt{M_{\pi\pi} M_\rho \Gamma_\rho}}{M_{\pi\pi}^2 - M_\rho^2 + i M_\rho \Gamma_\rho} + \frac{(A_\omega^R + i A_\omega^I)\sqrt{M_{\pi\pi} M_\omega \Gamma_{\omega\to\pi^+\pi^-}}}{M_{\pi\pi}^2 - M_\omega^2 + i M_\omega \Gamma_\omega} + \frac{(A_{f_2}^R + i A_{f_2}^I)\sqrt{M_{\pi\pi} M_{f_2} \Gamma_{f_2\to\pi^+\pi^-}}}{M_{\pi\pi}^2 - M_{f_2}^2 + i M_{f_2} \Gamma_{f_2}} + \frac{(A_{\rho(1700)}^R + i A_{\rho(1700)}^I)\sqrt{M_{\pi\pi} M_{\rho(1700)} \Gamma_{\rho(1700)\to\pi^+\pi^-}}}{M_{\pi\pi}^2 - M_{\rho(1700)}^2 + i M_{\rho(1700)} \Gamma_{\rho(1700)}} + B_{\pi\pi} \right|^2$$

Where $\Gamma_X = \Gamma_{0,X} \frac{M_X}{M_{\pi\pi}} \left(\frac{M_{\pi\pi}^2 - 4m_\pi^2}{M_X^2 - 4m_\pi^2} \right)^{2j+1/2}$ and $\Gamma_{X\to\pi\pi} = Br(X \to \pi\pi)\Gamma_X$

Orange: Relativisitic Breit-Wigner distributions.
Blue: Drell-Söding process modeled as a constant.

Previous results use a function like this, but struggle to differentiate the heavier resonances.

Simultaneous Fit Procedure

- In this formulation, fit the invariant mass spectrum, $A_{1\Delta\phi}$, $A_{2\Delta\phi}$, and $A_{3\Delta\phi}$.

  - $A_{1,3\Delta\phi} = (\frac{\rho\times f_2}{total}\times A_{1,3\Delta\phi}^{\rho\times f_2}) + (\frac{B_{\gamma A\rightarrow\pi\pi}\times f_2}{total}\times A_{1,3\Delta\phi}^{B_{\gamma A\rightarrow\pi\pi}\times f_2})$

- $A_{2\Delta\phi} = \left(\frac{\rho^2}{total}\times A_{2\Delta\phi}^{\rho^2}\right) + \left(\frac{B_{\gamma A\rightarrow\pi\pi}\times\rho}{total}\times A_{2\Delta\phi}^{B_{\gamma A\rightarrow\pi\pi}\times\rho}\right) + \left(\frac{B_{\gamma A\rightarrow\pi\pi}^2}{total}\times A_{2\Delta\phi}^{B_{\gamma A\rightarrow\pi\pi}^2}\right) + \left(\frac{\rho(1700)\times\rho}{total}\times A_{2\Delta\phi}^{\rho(1700)\times\rho}\right) + \left(\frac{B_{\gamma A\rightarrow\pi\pi}\times\rho(1700)}{total}\times A_{2\Delta\phi}^{B_{\gamma A\rightarrow\pi\pi}\times\rho(1700)}\right)$

Simultaneous Fit: $dN/dM_{\pi\pi}$

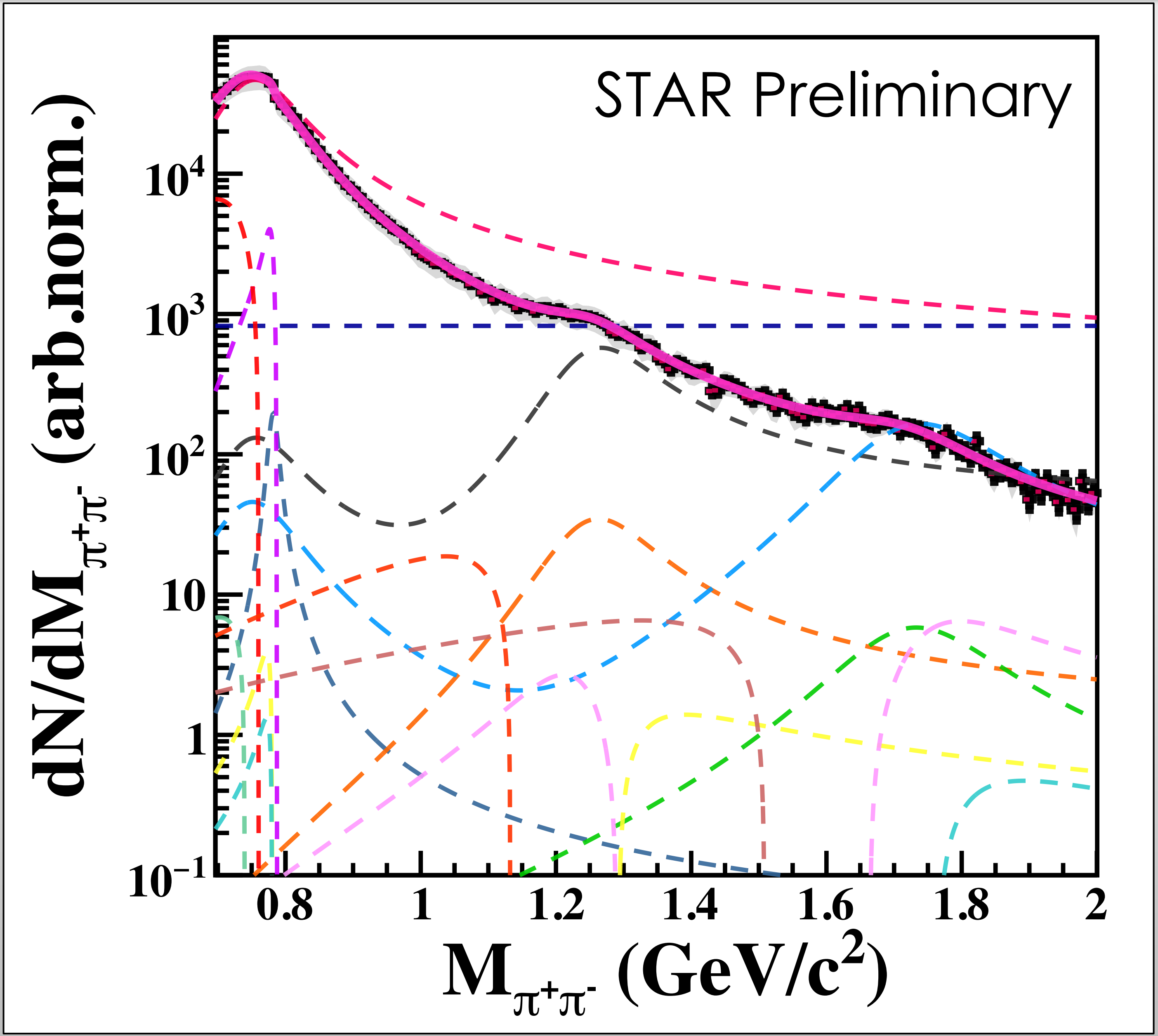

Invariant mass fit constrained by $A_{n\Delta\phi}$

Simultaneous Fit: $A_{1\Delta\phi}$

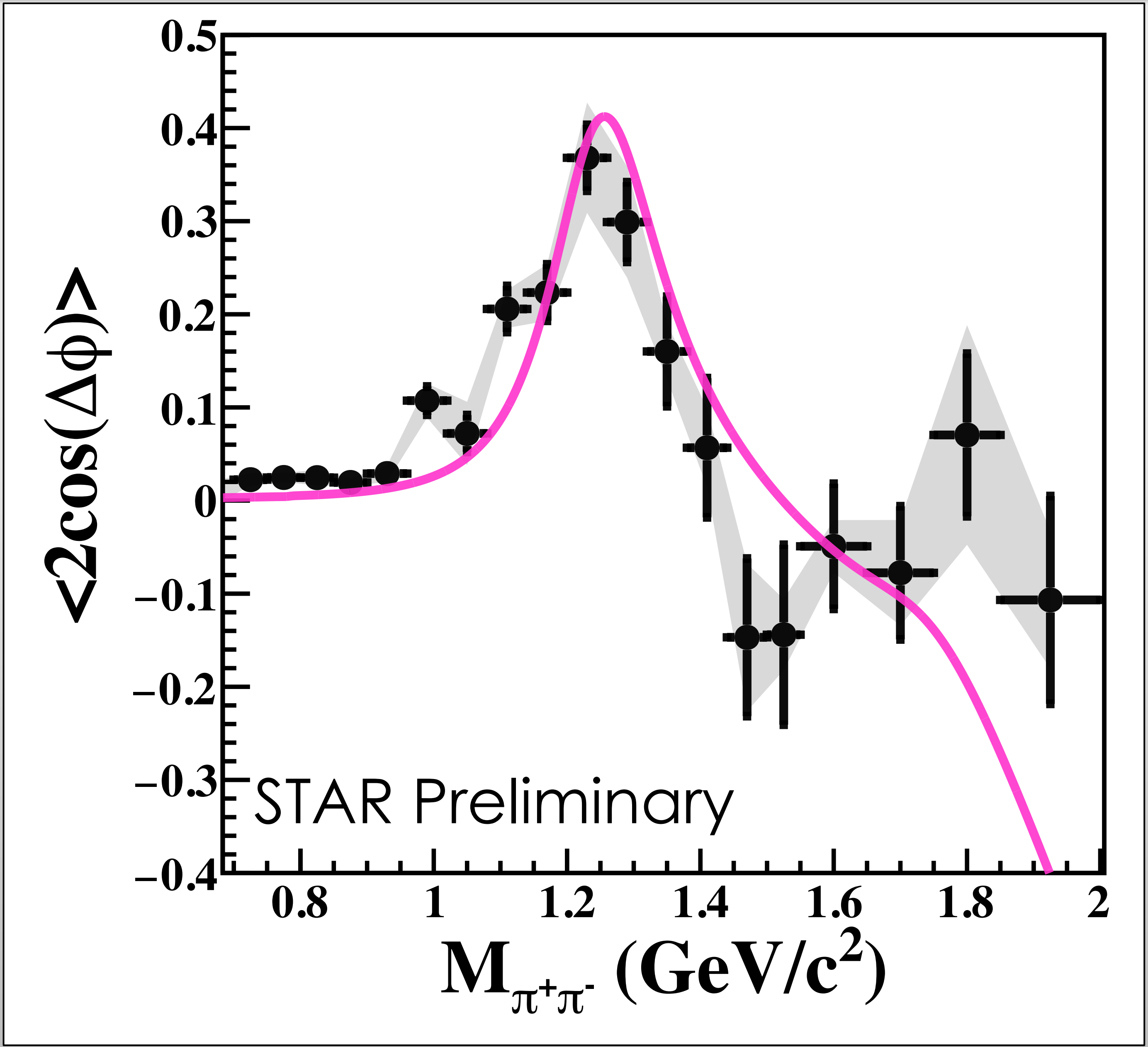

Contributions from:

- $\rho^0 \times f_2(1270)$
- Drell-Söding$\times f_2(1270)$

Simultaneous Fit: $A_{3\Delta\phi}$

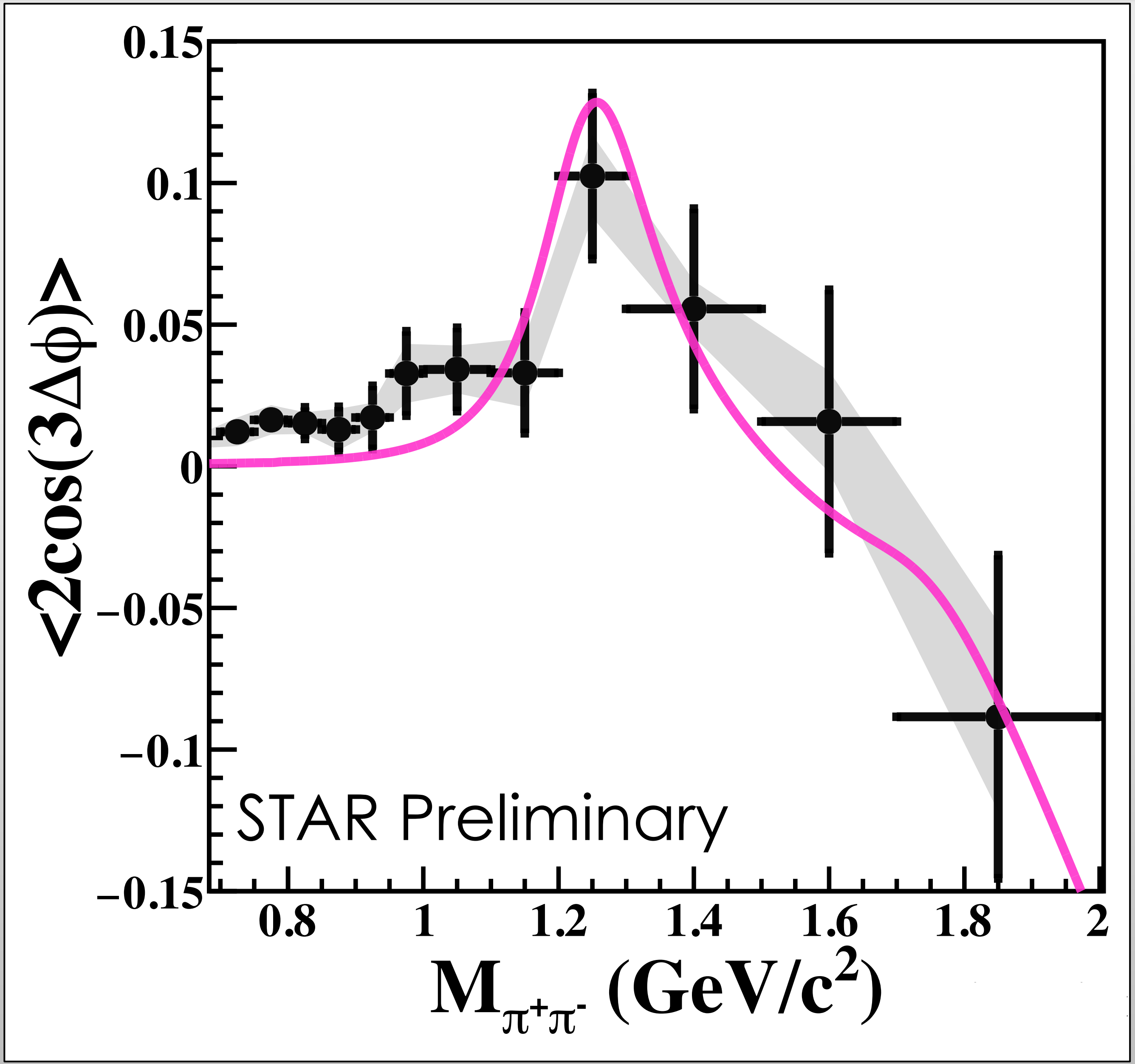

Contributions from:

- $\rho^0 \times f_2(1270)$
- Drell-Söding$\times f_2(1270)$

Simultaneous Fit

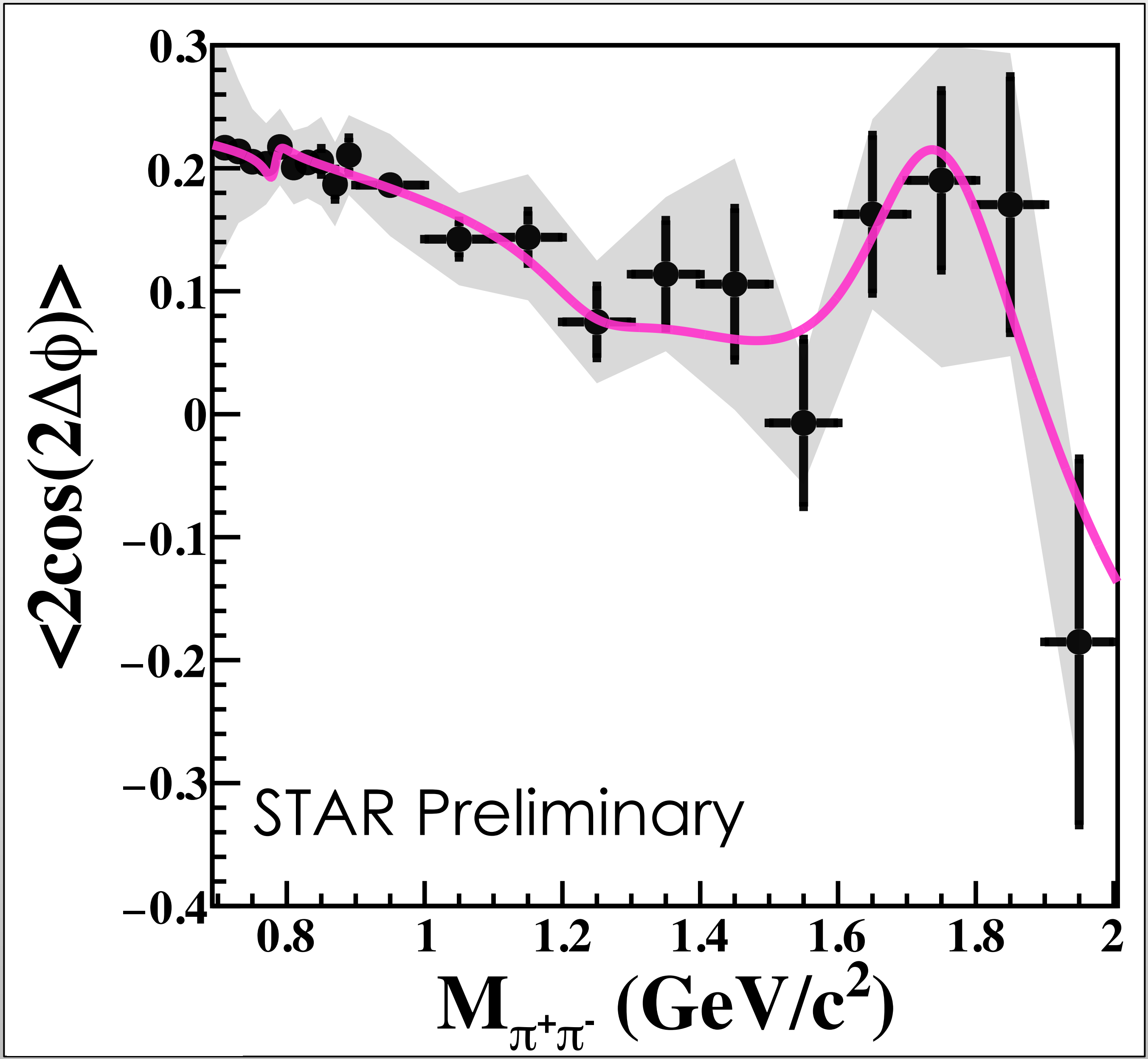

Contributions from:

- $\rho^0 \times \rho^0$
- Drell-Söding×Drell-Söding
- ρ^0×Drell-Söding
- $\rho^0 \times \rho(1700)$
- Drell-Söding×$\rho(1700)$

Simultaneous Fit

$$\frac{\chi^2}{ndf} = 2.9$$

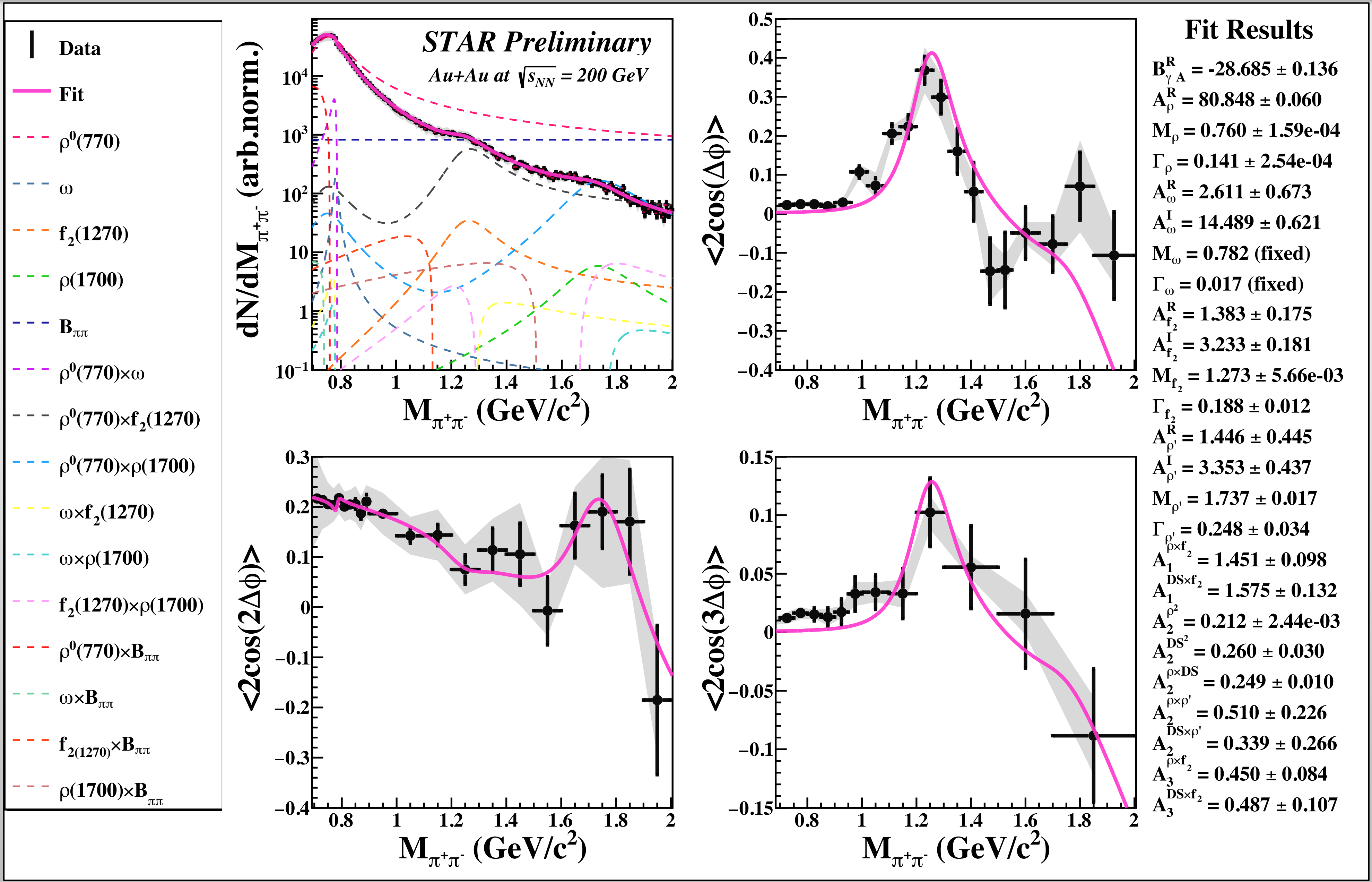

Tabulated Results

This fit (STAR Preliminary)

$M_\rho = 760.4 \pm 0.16 \pm 11 \frac{MeV}{c^2}$	$M_{f_2(1270)} = 1272.4 \pm 5.6 \pm 44 \frac{MeV}{c^2}$
$\Gamma_\rho = 142.0 \pm 0.25 \pm 14\ MeV$	$\Gamma_{f_2(1270)} = 188.5 \pm 11.6 \pm 115\ MeV$
$M_\omega = 782 \frac{MeV}{c^2}$ (fixed)	$M_{\rho(1700)} = 1737.3 \pm 17.3 \pm 71 \frac{MeV}{c^2}$
$\Gamma_\omega = 17\ MeV$ (fixed)	$\Gamma_{\rho(1700)} = 248.0 \pm 34 \pm 13\ MeV$

PDG mass, width:

$$M_{f_2(1270)} = 1275.5 \pm 0.8 \frac{MeV}{c^2}$$
$$\Gamma_{f_2(1270)} = 185.9 \pm 2.5\ MeV$$
$$M_{\rho(1700)} = 1720 \pm 20 \frac{MeV}{c^2}$$
$$\Gamma_{\rho(1700)} = 250 \pm 100\ MeV$$

ω fixed to results from STAR, Phys. Rev. C 96, 054904 (2017)

Results reported as: $value \pm statistical\ uncertainty \pm systematic\ uncertainty$

- Spin interference parameters constrain on the mass and width of $f_2(1270)$ and $\rho(1700)$.
  - Close agreement with PDG values for $f_2(1270)$.
  - $\rho(1700)$ width from this fit has smaller uncertainty than PDG (2022).

R.L. Workman et al. (Particle Data Group), Prog. Theor. Exp. Phys. 2022, 083C01 (2022)

Non-resonant $\gamma\gamma \rightarrow \pi^+\pi^-$

- Non-resonant $\gamma\gamma \rightarrow \pi^+\pi^-$ not included in fit.
- Largest contribution to $A_{1\Delta\phi}$ and $A_{3\Delta\phi}$ around ρ^0 mass.
- **Excess in data compared to fit in this region as a result.**

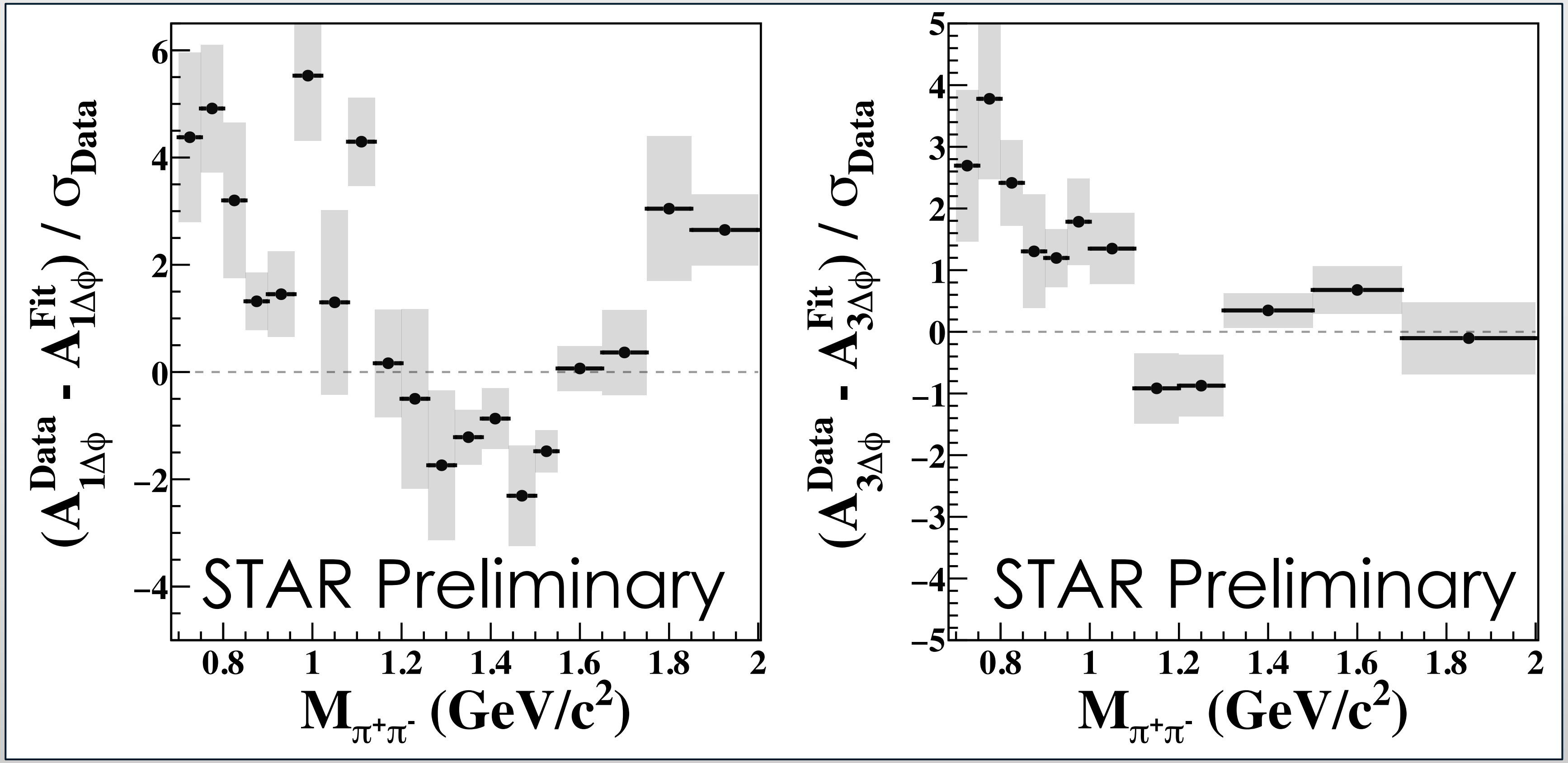

Conclusions

- $A_{1\Delta\phi}$ and $A_{3\Delta\phi}$ were measured for the first time in STAR Au+Au UPCs at 200 GeV.
  - **Spin interference between $\boldsymbol{\gamma A \rightarrow \pi^+\pi^-}$ and $\boldsymbol{\gamma\gamma \rightarrow \pi^+\pi^-}$.**
  - $A_{1\Delta\phi}$ and $A_{3\Delta\phi}$ **constrain $\boldsymbol{\gamma\gamma \rightarrow \pi^+\pi^-}$** cross section, phase (Hagiwara et al., Phys. Rev. D 103, 074013 (2021)).
  - $A_{1\Delta\phi}$ and $A_{3\Delta\phi}$ feature at ~1270 MeV/c^2 **indicates $\boldsymbol{\gamma\gamma \rightarrow f_2(1270) \rightarrow \pi^+\pi^-}$.**

- $A_{2\Delta\phi}$ as a function of $M_{\pi\pi}$ was also measured in the same system for the first time.

- The $A_{n\Delta\phi}$ and $\frac{dN}{dM_{\pi\pi}}$ were fit simultaneously with a **new technique that distinguishes resonances on $\boldsymbol{\frac{dN}{dM_{\pi\pi}}}$ according to their spin.**
  - Extracted values of the mass and width of $f_2(1270)$ and $\rho(1700)$.
  - Values of $f_2(1270)$ consistent with known results **confirms $\boldsymbol{\gamma\gamma \rightarrow \pi^+\pi^-}$ in UPC.**
  - **Next step: extract $\boldsymbol{d\sigma_{\gamma\gamma\rightarrow\pi^+\pi^-}/dM_{\pi\pi}}$**

References

STAR, Phys. Rev. C 96, 054904 (2017)

First Results from Fermilab's Muon g-2 Experiment Strengthen Evidence of New Physics; Fermilab, 7 April 2021.

Danilkin, C. F. Redmer, and M. Vanderhaeghen, Prog. Part. Nucl. Phys. 107, 20 (2019).

Daniel Melo-Porras, Edilson Alfonso Reyes Rojas, Angelo Raffaele Fazio, Particles 2024, 7(2), 327 – 381

Brandenburg, Duan, Tu, Venugopalan, and Xu, Phys. Rev. Research 7, 013131 (2025)

STAR, Sci.Adv.9,eabq3903 (2023)

Hagiwara, Zhang, Zhou, and Zhou, Phys. Rev. D 103, 074013 (2021)